Kinetics of restricted solid-on-solid models of film growth

J. W. Evans[1] and M. C. Bartelt[2]
[1]*Department of Mathematics and Ames Laboratory, Iowa State University, Ames, Iowa 50011*
[2]*Institute for Physical Research and Technology, Iowa State University, Ames, Iowa 50011*
(Received 11 June 1993; revised manuscript received 2 August 1993)

We consider the kinetics of irreversible film growth in solid-on-solid models with various restrictions on the adsorption (or growth) sites. We show how the master equations for the probabilities of subconfigurations of filled sites can be analyzed exactly to obtain coverages and spatial correlations for the first several layers. These provide an efficient framework for analysis of the early-stage growth kinetics, and indicate rapid attainment of asymptotic behavior. We illustrate the (1+1)- and (2+1)-dimensional cases for the simplest restricted solid-on-solid condition, and various modifications.

PACS number(s): 05.40.+j, 68.55.−a, 05.70.Ln

I. INTRODUCTION

Theoretical effort toward understanding the nonequilibrium growth of thin films has intensified in recent years. The emphasis has been on the asymptotic behavior of the roughness and height-height correlation functions [1]. In contrast, much of the experimental interest is in the early stages of growth of ultrathin films [2]. Our analysis of restricted solid-on-solid (RSOS) models [3] shifts the focus from the asymptotics to the initial growth kinetics. Adopting an approach used previously for single-step models [4], we show how exact (finite) closed sets of rate equations can be obtained for the layer coverages and for more complicated subconfiguration probabilities. Since the number of such equations increases dramatically with layer height, these are only analyzed explicitly for the first several layers in $d=1+1$ and $2+1$ dimensions. We emphasize that the exact results for higher layer coverages are nontrivial because of the correlated nature of the filling in these layers. Corresponding exact analysis is *not* possible in, e.g., the Eden and ballistic deposition models. Finally we note that since asymptotic behavior is achieved quickly in these models, knowledge of only the first several layer coverages suffices to give a fairly complete picture.

General RSOS models with simple cubic adsorption geometries allow random deposition of monomers in each layer, provided that the sites underneath the adsorption site and some additional set of their neighbors are occupied. This often corresponds to imposing a constraint on the height difference of adjacent columns of occupied sites. Thus, by construction, no film configurations with overhangs or lattice vacancies are generated, and the filling of any one layer is independent of all layers above. For the simplest of such models (hereafter referred to as *the standard RSOS model)* adsorption requires that the site directly beneath the adsorption site, and all its in-plane nearest neighbors, be occupied, i.e., the adsorption sites are selected from among those supported by a platform of three, five, etc., filled nearest sites in the layer underneath, in dimensions $d=1+1$, $2+1$, etc., respectively. Here the heights of two adjacent columns cannot differ by more than one unit (e.g., one layer). With this height constraint, the local slope of the film interface is bounded (by one in $d=1+1$; for $d\geq 2+1$ the value depends on direction). We will also comment on RSOS models with arbitrary height difference and platform size.

In a coarse-grained description of solid-on-solid models, the film configuration is assigned a stochastic height variable, $h(\mathbf{x},t)$, which is a single-valued function of the lateral position $\mathbf{x}$ and time t. This quantity satisfies a stochastic evolution equation of the form [5]

$$\frac{\partial h(\mathbf{x},t)}{\partial t}=fS(\nabla h,\nabla^2 h,\ldots)+\eta(\mathbf{x},t)\ . \tag{1}$$

Here f is a uniform deposition flux; S is the "sticking probability" which depends on the local slope, curvature, etc., and η is a zero-mean δ-function-correlated noise, so $\langle\eta\rangle=0$ and $\langle\eta(\mathbf{x},t)\eta(\mathbf{x}',t')\rangle=2D\delta(\mathbf{x}-\mathbf{x}')\delta(t-t')$. Clearly the RSOS adsorption-site concentration, and thus S, will *decrease* with increasing $|\nabla h|$, and S will be identically zero at the maximum allowed slope [5] (depending on the tilt direction in $d=2+1$). In fact, S also depends on the curvature, since one expects a higher density of RSOS adsorption sites at local minima of the interface than at local maxima [5]. Thus S should have the form $S=S_0+\lambda|\nabla h|^2+v\nabla^2 h+\cdots$, here $\lambda<0$ and $v>0$, reducing (1) to the so-called Kardar-Parisi-Zhang (KPZ) equation [6]. [Note that, starting with $S=S_0+\nabla h\cdot\underline{\lambda}\cdot\nabla h+(\nabla\cdot\underline{v}\cdot\nabla)h+\cdots$, symmetry arguments [5] show that $\underline{\lambda}$ and $\underline{v}$ are diagonal.] It should be emphasize that (1) applies to the regime where the interface is locally equilibrated, so S_0 is related to the nontrivial asymptotic growth velocity of the interface, and λ and v are likewise nontrivial.

Kim and co-workers [3] have reported on extensive simulations of the asymptotic kinetics of RSOS models from $2+1$ to $5+1$ dimensions, conjecturing on the values of the KPZ scaling exponents in all dimensions. Their conjecture is generally believed to be close but not exact [7]. Since our analysis is restricted to the early stage of growth, we cannot contribute to this discussion. However, we do analyze the short-time evolution of the standard deviation and skewness of the film-height distribution to-

ward the asymptotic KPZ behavior (at least in $d=1+1$ dimensions).

This work is organized as follows. In Sec. II we outline the basic method of generating the master equations for subconfiguration probabilities, and we apply it to the standard RSOS model in $1+1$ and $2+1$ dimensions. Results for basic quantities of interest are presented in Sec. III. Variations of the model to include different adsorption-site constraints, vicinal surfaces, and inhomogeneous deposition are discussed in Sec. IV. Section V is a summary.

II. THE MASTER EQUATIONS FOR AN INITIALLY FLAT SURFACE

For all thin-film growth models on infinite substrates, the master equations can be recast in the form of an infinite hierarchy of rate equations for the various subconfiguration probabilities (including the coverages). In the RSOS growth problem these sets of equations for any specific layer coverage can be closed exactly, as observed previously for different adsorption-site geometries [4]. This we illustrate next in $1+1$ and $2+1$ dimensions. We start with the simplest adsorption-site constraint described above (the standard RSOS model). Generalization of the formalism follows naturally.

Let $\theta_k(t)$ denote the probability of finding an occupied site in layer k (i.e., the coverage of layer k), and $S_k(t)$ that of finding an empty site *obeying the RSOS condition* in layer k, at time t. Then one has $d\theta_k/dt=S_k$, with the deposition flux f set to unity. At $t=0$, we set $\theta_k=0, \forall k\geq 1$, and $\theta_0=1$.

The occupation of the first layer is purely random in any dimension, and

$$S_1=1-\theta_1 \tag{2}$$

by conservation of probability. From the rate equation above, $d\theta_1/dt=S_1$, and one obtains $\theta_1=1-e^{-t}$ for an initially clean surface. For $k\geq 2$ it is notationally more convenient to separate the two cases $d=1+1$ and $d=2+1$.

A. $d=1+1$

Let k ($\underline{k}$) denote a filled (empty) layer-k site, and configurations of several such sites enclosed in square parentheses denote the corresponding probabilities. For instance, one has

$$\theta_2=[2]=\begin{bmatrix} & 2 & \\ 1 & 1 & 1 \end{bmatrix},\quad [2\underline{2}]=\begin{bmatrix} & 2 & \underline{2} \\ 1 & 1 & 1 \end{bmatrix},$$

etc. Using probability conservation for $k\geq 2$ gives

$$\begin{aligned} S_k &= \begin{bmatrix} & \underline{k} & \\ k-1 & k-1 & k-1 \end{bmatrix} \\ &= [k-1\ \ k-1\ \ k-1]-\begin{bmatrix} & k & \\ k-1 & k-1 & k-1 \end{bmatrix} \\ &= [k-1\ \ k-1\ \ k-1]-\theta_k\ , \end{aligned} \tag{3}$$

to be compared with (2) for the first layer.

Now we develop the rate equations for the θ_k. The equation for $d\theta_1/dt$ was given above. For the second-layer coverage

$$\frac{d\theta_2}{dt}=S_2=[1\ 1\ 1]-\theta_2=\theta_1^3-\theta_2\ , \tag{4}$$

using $[1\ 1\ 1]=\theta_1^3$, since the first layer is randomly occupied. For the third-layer coverage,

$$\frac{d\theta_3}{dt}=S_3=[2\ 2\ 2]-\theta_3\ , \tag{5}$$

which introduces the first nontrivial quantity $[2\ 2\ 2]$, whose rate equation has the form

$$\frac{d[2\ 2\ 2]}{dt}=2\begin{bmatrix} & \underline{2} & 2 & 2 & \\ 1 & 1 & 1 & 1 & 1 \end{bmatrix}+\begin{bmatrix} & 2 & \underline{2} & 2 & \\ 1 & 1 & 1 & 1 & 1 \end{bmatrix}. \tag{6}$$

Here one can use the identities

$$\begin{aligned} \begin{bmatrix} & \underline{2} & 2 & 2 & \\ 1 & 1 & 1 & 1 & 1 \end{bmatrix}+[2\ 2\ 2] &= \begin{bmatrix} & & 2 & 2 & \\ 1 & 1 & 1 & 1 & 1 \end{bmatrix} \\ &= [1]\begin{bmatrix} & 2 & 2 & \\ 1 & 1 & 1 & 1 \end{bmatrix} \\ &= [1][2\ 2] \end{aligned} \tag{7}$$

(where factorization is possible because first layer sites are filled randomly), and

$$[2\ \underline{2}\ 2]+[2\ 2\ 2]=[2\_\_2]\ , \tag{8}$$

the "__" representing a RSOS adsorption site of unspecified occupancy. One finally obtains

$$\frac{d[2\ 2\ 2]}{dt}=2[1][2\ 2]+[2\_\_2]-3[2\ 2\ 2]\ . \tag{9}$$

Next we need to consider the rate equations for $[2\ 2]$ and $[2\_\_2]$, which have the form

$$\frac{d[2\ 2]}{dt}=2\begin{bmatrix} & \underline{2} & 2 & \\ 1 & 1 & 1 & 1 \end{bmatrix}, \tag{10}$$

and

$$\frac{d[2\_\_2]}{dt}=2\begin{bmatrix} & \underline{2} & & 2 & \\ 1 & 1 & 1 & 1 & 1 \end{bmatrix}. \tag{11}$$

Here we use

$$\begin{aligned} \begin{bmatrix} & \underline{2} & 2 & \\ 1 & 1 & 1 & 1 \end{bmatrix}+[2\ 2] &= \begin{bmatrix} & & 2 & \\ 1 & 1 & 1 & 1 \end{bmatrix} \\ &= [1]\begin{bmatrix} & 2 & \\ 1 & 1 & 1 \end{bmatrix}=[1][2]\ , \end{aligned} \tag{12}$$

and

$$\begin{aligned} \begin{bmatrix} & \underline{2} & & 2 & \\ 1 & 1 & 1 & 1 & 1 \end{bmatrix}+[2\_\_2] &= \begin{bmatrix} & & & 2 & \\ 1 & 1 & 1 & 1 & 1 \end{bmatrix} \\ &= [1]^2\begin{bmatrix} & 2 & \\ 1 & 1 & 1 \end{bmatrix}=[1]^2[2]\ . \end{aligned} \tag{13}$$

Combining (10)–(13) finally gives

$$\frac{d[2\ 2]}{dt}=2([1][2]-[2\ 2])\ , \tag{14}$$

and

$$\frac{d[2\_\_2]}{dt}=2([1]^2[2]-[2\_\_2])\ . \tag{15}$$

One could easily continue to moderate values of k. However, the number of closed coupled equations needed to determine θ_k increases rapidly with the layer index: one equation for $k=1$, two for $k=2$, then 6, 20, and 99 equations, for $k=3$, 4, and 5, respectively. We have obtained these equations for $k\leq 5$, and in Sec. III show results from their analysis.

B. $d=2+1$

As we indicated before, for the first layer $d\theta_1/dt=S_1=1-\theta_1$ applies. For layers $k\geq 2$, probability conservation gives

$$S_k=\begin{bmatrix} & k-1 & \\ k-1 & k-1 & k-1 \\ & k-1 & \end{bmatrix}-\theta_k\ , \tag{16}$$

in a *top view* of the lattice. The number of closed coupled rate equations, necessary to determine the coverages, increases from one for $k=1$ and 2, to nine for $k=3$, and to over 1000 for $k=4$. The following is the complete set of equations for the second and third layers:

$$\frac{d\theta_2}{dt}=\begin{bmatrix} & 1 & \\ 1 & 1 & 1 \\ & 1 & \end{bmatrix}-\theta_2=[1]^5-\theta_2\ , \tag{17a}$$

$$\frac{d\theta_3}{dt}=\begin{bmatrix} & 2 & \\ 2 & 2 & 2 \\ & 2 & \end{bmatrix}-\theta_3\ , \tag{17b}$$

$$\frac{d\begin{bmatrix} & 2 & \\ 2 & 2 & 2 \\ & 2 & \end{bmatrix}}{dt}$$

$$=4\begin{bmatrix} & \underline{2} & \\ 2 & 2 & 2 \\ & 2 & \end{bmatrix}+\begin{bmatrix} & 2 & \\ 2 & \underline{2} & 2 \\ & 2 & \end{bmatrix}$$

$$=4[1]\begin{bmatrix} 2 & 2 & 2 \\ & 2 & \end{bmatrix}+\begin{bmatrix} & 2 & \\ 2 & & 2 \\ & 2 & \end{bmatrix}-5\begin{bmatrix} & 2 & \\ 2 & 2 & 2 \\ & 2 & \end{bmatrix}\ , \tag{17c}$$

$$\frac{d\begin{bmatrix} 2 & 2 & 2 \\ & 2 & \end{bmatrix}}{dt}$$

$$=2\begin{bmatrix} \underline{2} & 2 & 2 \\ & 2 & \end{bmatrix}+\begin{bmatrix} 2 & 2 & 2 \\ & \underline{2} & \end{bmatrix}+\begin{bmatrix} 2 & \underline{2} & 2 \\ & 2 & \end{bmatrix}$$

$$=2[1]^2\begin{bmatrix} 2 & 2 \\ 2 & \end{bmatrix}+[1][2\ 2\ 2]$$

$$+[1]\begin{bmatrix} 2 & & 2 \\ & 2 & \end{bmatrix}-4\begin{bmatrix} 2 & 2 & 2 \\ & 2 & \end{bmatrix}\ , \tag{17d}$$

TABLE I. The nonzero polynomials $Q_m^{(k)}$ for $1\leq k\leq 4$, in $d=1+1$.

$Q_0^{(1)}=1$
$Q_1^{(1)}=-1$
$Q_0^{(2)}=1$
$Q_1^{(2)}=\frac{3}{2}-3t$
$Q_2^{(2)}=-3$
$Q_3^{(2)}=\frac{1}{2}$
$Q_0^{(3)}=1$
$Q_1^{(3)}=-\frac{37}{3}+13t-9t^2/2$
$Q_2^{(3)}=-\frac{22}{3}+16t-12t^2$
$Q_3^{(3)}=\frac{25}{2}+6t-9t^2/2+t^3$
$Q_4^{(3)}=\frac{19}{3}$
$Q_5^{(3)}=-\frac{1}{6}$
$Q_0^{(4)}=1$
$Q_1^{(4)}=15\,811\,529/207\,360-673t/8+129t^2/4-9t^3/2$
$Q_2^{(4)}=-55\,243\,169/194\,400+149\,443t/360-1175t^2/4+203t^3/2-67t^4/4$
$Q_3^{(4)}=1\,375\,673/3456-149\,417t/288+6931t^2/24-5783t^3/48+1805t^4/32-153t^5/16+163t^6/240$
$Q_4^{(4)}=-48\,023/648+361t/36-335t^2/36-85t^3/3+65t^4/6$
$Q_5^{(4)}=-13\,503\,439/124\,416-103\,309t/10\,368+4361t^2/1728-311t^3/216+175t^4/288-t^5/15$
$Q_6^{(4)}=-36\,823/4320$
$Q_7^{(4)}=9217/259\,200$

TABLE II. The nonzero polynomials $Q_m^{(k)}$ for $1 \le k \le 3$, in $d = 2+1$.

$Q_0^{(1)} = 1$
$Q_1^{(1)} = -1$
$Q_0^{(2)} = 1$
$Q_1^{(2)} = \frac{65}{12} - 5t$
$Q_2^{(2)} = -10$
$Q_3^{(2)} = 5$
$Q_4^{(2)} = -\frac{5}{3}$
$Q_5^{(2)} = \frac{1}{4}$
$Q_0^{(3)} = 1$
$Q_1^{(3)} = -42\,153\,211\,543/1\,143\,072\,000 + 107t/2 - 25t^2/2$
$Q_2^{(3)} = -42\,148/105 + 1184t/3 - 160t^2$
$Q_3^{(3)} = -113\,408\,171/58\,800 + 1\,014\,907t/420 - 2163t^2/2 + 190t^3$
$Q_4^{(3)} = -1\,859\,891\,263/514\,500 + 207\,413\,614t/33\,075 - 3\,100\,576t^2/945 + 2624t^3/3 - 880t^4/9$
$Q_5^{(3)} = 136\,245\,621\,307\,949/31\,116\,960\,000 + 10\,809\,752\,897t/6\,174\,000 - 207\,388\,711t/132\,300 + 2\,402\,741t^3/3780 - 2227t^4/18 + 31t^5/3$
$Q_6^{(3)} = 4\,743\,707/2250 - 79514t/75 + 2012t^2/5 - 48t^3$
$Q_7^{(3)} = -804\,323/1296 + 33\,001t/162 - 65t^2/3$
$Q_8^{(3)} = 39\,930\,286/297\,675 - 9760t/567$
$Q_9^{(3)} = -14\,773\,057/672\,000 + 29t/48$
$Q_{10}^{(3)} = 128\,085\,697/44\,651\,250$
$Q_{11}^{(3)} = -12\,304\,751/41\,674\,500$
$Q_{12}^{(3)} = 9383/432\,180$
$Q_{13}^{(3)} = -17/20\,736$

$$\frac{d\left[\begin{smallmatrix} & 2 & \\ 2 & & 2 \\ & 2 & \end{smallmatrix}\right]}{dt} = 4\left[\begin{smallmatrix} & \underline{2} & \\ 2 & & 2 \\ & 2 & \end{smallmatrix}\right] = 4[1]^2\left[\begin{smallmatrix} 2 & & 2 \\ & 2 & \end{smallmatrix}\right] - 4\left[\begin{smallmatrix} & 2 & \\ 2 & & 2 \\ & 2 & \end{smallmatrix}\right], \tag{17e}$$

$$\frac{d\left[\begin{smallmatrix} 2 & 2 \\ & 2 \end{smallmatrix}\right]}{dt} = 2\left[\begin{smallmatrix} \underline{2} & 2 \\ & 2 \end{smallmatrix}\right] + \left[\begin{smallmatrix} 2 & 2 \\ & \underline{2} \end{smallmatrix}\right] = 2[1]^3\left[\begin{smallmatrix} & 2 \\ 2 & \end{smallmatrix}\right] + [1]^2[2\_\_2] - 3\left[\begin{smallmatrix} 2 & & 2 \\ & 2 & \end{smallmatrix}\right], \tag{17f}$$

$$\frac{d\left[\begin{smallmatrix} 2 & 2 \\ 2 & \end{smallmatrix}\right]}{dt} = \left[\begin{smallmatrix} \underline{2} & 2 \\ 2 & \end{smallmatrix}\right] + 2\left[\begin{smallmatrix} 2 & \underline{2} \\ 2 & \end{smallmatrix}\right] = [1]^2\left[\begin{smallmatrix} & 2 \\ 2 & \end{smallmatrix}\right] + 2[1]^2[2\ 2] - 3\left[\begin{smallmatrix} 2 & 2 \\ 2 & \end{smallmatrix}\right], \tag{17g}$$

$$\frac{d\left[\begin{smallmatrix} & 2 \\ 2 & \end{smallmatrix}\right]}{dt} = 2\left[\begin{smallmatrix} & 2 \\ \underline{2} & \end{smallmatrix}\right] = 2[1]^3[2] - 2\left[\begin{smallmatrix} & 2 \\ 2 & \end{smallmatrix}\right], \tag{17h}$$

$$\frac{d[2\_\_2]}{dt} = 2[2\_\_2] = 2[1]^4[2] - 2[2\_\_2], \tag{17i}$$

and

$$\frac{d[2\ 2]}{dt} = 2[\underline{2}\ 2] = 2[1]^3[2] - 2[2\ 2]. \tag{17j}$$

Results from analysis of these are shown in Sec. III.

As a final observation, we note that the exact solutions of these rate equations for the layer coverages can be written as a finite sum of the form

$$\theta_k(t) = \sum_{m=0}^{N(k)} Q_m^{(k)}(t)\, e^{-mt}, \tag{18}$$

where the coefficients $Q_m^{(k)}$ are dimension- and layer-dependent polynomials in t (see also Tables I and II). Note that for an initially clean surface the $Q_m^{(k)}$ satisfy the condition $\sum_m Q_m^{(k)}(0) = 0$, for fixed k. Since $\theta_k \to 1$ as $t \to \infty$, one also has $Q_0^{(k)}(t) = 1$ for all k and d. $N(k)$, the upper limit of the summation index, gives the fastest decaying exponential in (18). It equals the minimum number of filled sites in the first layer (i.e., the platform size) required to support a filled site in layer k. Thus, for the standard RSOS model, one finds, e.g., that $N(k) = 2k - 1$ for $d = 1+1$, and $N(k) = 2k(k-1)+1$ for $d = 2+1$.

III. RESULTS

Here we integrate the closed sets of rate equations described above to obtain exactly the first several layer coverages. These are used to obtain estimates of basic quantities which depend on all the layer coverages, e.g., the film height and growth rate, the interface width and skewness. However, for the range of times considered, the higher layer coverages neglected are essentially zero [$< O(10^{-8})$], so the results for the latter quantities are

essentially exact.

Figure 1 shows the first several layer coverages, and the average film height (or total coverage), $h=\sum_{k(\geq 1)}\theta_k$, as functions of time. The height is asymptotically linear in time. Figure 2 shows the individual layer growth rates $d\theta_k/dt$, and the total growth rate $R(t)=dh/dt=\sum_{k(\geq 1)}d\theta_k/dt$. $R(t)$ equals the total density of growth sites. We estimate its asymptotic value at $R(\infty)\sim 0.43\pm 0.02$ in $d=1+1$, and $R(\infty)\sim 0.32\pm 0.03$ in $d=2+1$ (see the insets in Fig. 2). The first value is consistent with previous simulation estimates [8,9] which yield ~ 0.42. To obtain these asymptotic values we exploit the scaling results of Krug and Meakin [10]. They show that scaling in the form $R(\infty)-R(t)\sim t^{-2/3}$ holds in $d=1+1$. This relation allows more accurate extrapolation of $R(\infty)$ [see in the inset in Fig. 2(a)]. In $d=2+1$, they estimate [10] that $R(\infty)-R(t)\sim t^{-0.77}$ as used in Fig. 2(b).

Other basic quantities of interest involve the distribution $E_k=\theta_k-\theta_{k+1}$ of exposed surface sites in layer k (recalling that $\theta_0\equiv 1$ here, so $E_k=0$ for $k<0$). These include the surface scattered Bragg intensity at the antiphase condition (where scattering from consecutive layers interferes destructively) defined as

$$I_{\text{Bragg}}(t)=\left[\sum_{k=0}^{\infty}(-1)^k E_k(t)\right]^2, \tag{19}$$

the film interface width

$$w^2(t)=\sum_{k=0}^{\infty}[k-h(t)]^2 E_k(t), \tag{20}$$

and the skewness of the distribution E_k,

$$S(t)=\frac{\sum_{k=0}^{\infty}[k-h(t)]^3 E_k(t)}{\left\{\sum_{k=0}^{\infty}[k-h(t)]^2 E_k(t)\right\}^{3/2}}. \tag{21}$$

Figure 3 shows the antiphase Bragg intensities. Clearly the film is smoother in $2+1$ dimensions, where oscillations are longer lived. The interface width and the skewness are shown in Fig. 4. Asymptotically one expects [1] $w^2\sim t^{2\beta}$ and [9] $S(t)\sim$ constant. In one dimension the

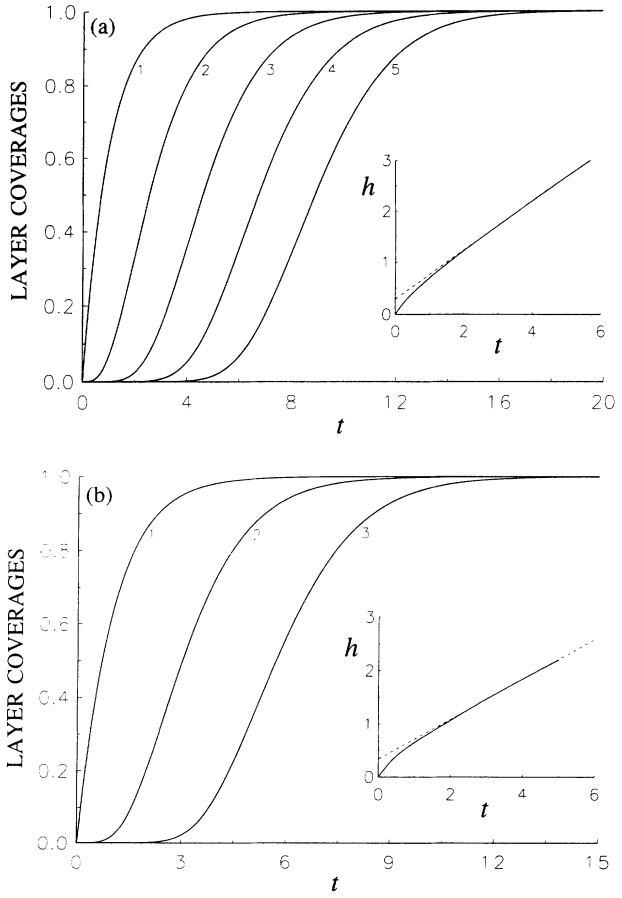

FIG. 1. The layer coverages (labeled by layer index) as functions of time t (in units of the inverse of the flux rate). In (a) $d=1+1$, and in (b) $d=2+1$. The insets show the linear behavior in time of the film height h (in monolayers), after deposition of a few layers.

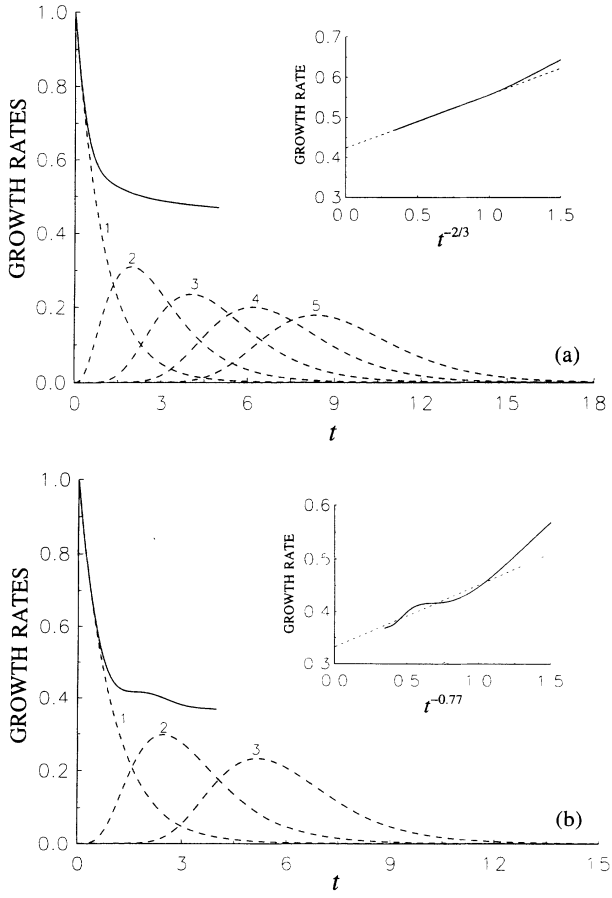

FIG. 2. The total growth rate (solid curve) and the individual-layer growth rates (dashed curves, labeled by layer index) in (a) $d=1+1$, and (b) $d=2+1$. In the insets, the large time scaling [10] of the total growth rate (solid curve) is exploited.

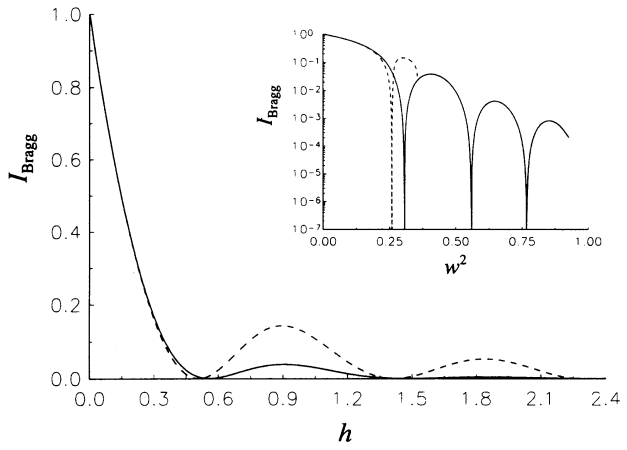

FIG. 3. The antiphase Bragg intensities I_{Bragg} (normalized to unity for a clean substrate) as functions of the film height h (in monolayers) in $d=1+1$ (solid line) and $2+1$ (dashed line). The inset shows the intensities in terms of the corresponding interface widths, w^2. The envelope of the oscillations scales [5] exponentially with w^2 for large w.

five-layer estimate of $\beta=0.33\pm0.01$ (from the $\ln w-\ln t$ slope) is close to the exact value [6] ($\frac{1}{3}$), but caution is needed in general in assessing such early estimates as representative of the asymptotic scaling. The skewness (shown in the insets) is asymptotically negative, as expected for RSOS models in any dimension. For one-dimensional KPZ models, Krug, Meakin, and Halpin-Healy [9] estimated the asymptotic value $S(\infty)=-0.28\pm0.04$, consistent with our results.

Analysis of height-height correlations is also of interest. One can start with the probabilities $P_{ij}(\mathbf{x},t)$ that two sites, in layers i and j, separated laterally by $\mathbf{x}$, are

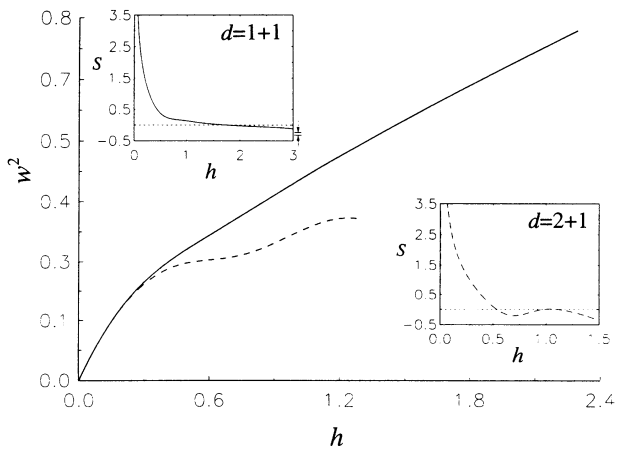

FIG. 4. The square of the interface width, w^2, in terms of the film height h (in monolayers): $d=1+1$ (solid line) and $2+1$ (dashed line). The $2+1$-dimensional data has not reached the scaling region. The insets show the skewness S of the distribution of exposed surface sites, as a function of the film height. We also indicate the range of the asymptotic value estimated in Ref. [9] for $d=1+1$.

occupied at time t. From these and simple probability conservation, one can construct the probabilities $Q_{ij}(\mathbf{x},t)$ that two filled sites in layers i and j, separated laterally by $\mathbf{x}$, are *not* covered by higher layers at time t. One obtains $Q_{ij}(\mathbf{x},t)=P_{ij}(\mathbf{x},t)-P_{ij+1}(\mathbf{x},t)-P_{i+1j}(\mathbf{x},t)+P_{i+1j+1}(\mathbf{x}t)$. The height-height correlation function is simply $G(\mathbf{x},t)\propto\sum_{ij}(i-j)^2Q_{ij}(\mathbf{x},t)$, which scales as $|\mathbf{x}|^{2\alpha}$, as $t\to\infty$, for large $|\mathbf{x}|$. Analysis of G can in principle be done analytically for moderate t, but in practice simulations would be more efficient.

IV. VARIATIONS OF THE STANDARD RSOS MODEL

A. Vicinal surfaces

The above formulation can be extended to analyze RSOS growth models on initially perfect vicinal surfaces. Figure 5 shows a schematic of an example in $d=1+1$, treated here in some detail, and serves to elucidate the basic approach. Restricted translational invariance forces the sites in Fig. 5 with distinct labels to have distinct occupancies and growth rates, and so must be treated accordingly. Let $\theta_1(t),\theta_2(t),\ldots$ be the probabilities that sites labeled $1,2,\ldots,$ respectively, are filled at time t. We start with $\theta_1(0)=\theta_2(0)=\cdots=0$. The heights of columns $A\equiv\{1,3,5,7,\ldots\}$ and $B\equiv\{2,4,6,8,\ldots\}$ are given by $h_A=\theta_1+\theta_3+\theta_5+\cdots$ and $h_B=\theta_2+\theta_4+\theta_6+\ldots$, respectively, with $0<h_A-h_B<1$ at all times. One is interested, e.g., in the growth rates $R_A(t)=dh_A/dt$ and $R_B(t)=dh_B/dt$, and their common asymptotic value $R(\infty)=R_A(\infty)=R_B(\infty)$. Note that $R_A>R_B$ for all finite t, with R_A-R_B vanishing faster than $1/t$, as $t\to\infty$, since $\int_0^\infty(R_A-R_B)dt=\lim_{t\to\infty}(h_A-h_B)<1$.

As before, we fix the deposition flux at unity. Rate equations for the labeled-site occupation probabilities, obtained via enumeration of configurations, exploit again probability conservation. In general, let $[\underline{k}]$ represent the probability that a site with label k (cf. Fig. 5) is empty, while $[k]$ represents the probability for a filled site ($k=0$ corresponds to substrate sites, so $[0]\equiv1$ at all times). Clearly, filling of 1-sites satisfies

$$\frac{d\theta_1}{dt}=\begin{bmatrix}\underline{1}\\0\ 0\ 0\end{bmatrix}=1-\begin{bmatrix}1\\0\ 0\ 0\end{bmatrix}=1-\theta_1\ . \tag{22}$$

The rate of change of θ_2 depends on θ_1 via

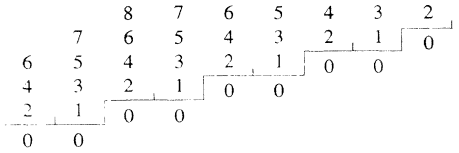

FIG. 5. The distinct growth sites on a perfect vicinal surface with initial slope $\frac{1}{2}$, in $1+1$ dimensions. Sites with the same label are kinetically equivalent.

$$\frac{d\theta_2}{dt}\begin{bmatrix} \underline{2} \\ 1\ 0\ 0 \end{bmatrix}=[1\ 0\ 0]-\begin{bmatrix} 2 \\ 1\ 0\ 0 \end{bmatrix}=\theta_1-\theta_2\ . \tag{23}$$

Continuing to $k=3$,

$$\frac{d\theta_3}{dt}=\begin{bmatrix} \underline{3} \\ 2\ 1\ 0 \end{bmatrix}=[2\ 1\ 0]-\begin{bmatrix} 3 \\ 2\ 1\ 0 \end{bmatrix}$$
$$=[2\ 1]-\theta_3=\theta_1\theta_2-\theta_3\ , \tag{24}$$

noting that the occupancy of the adjacent sites 2 and 1 (see Fig. 5) is uncorrelated, as proved by the relation

$$\frac{d[2\ 1]}{dt}=\begin{bmatrix} \underline{2}\ 1 \\ 1\ 0\ 0\ 0 \end{bmatrix}+\begin{bmatrix} 2\ \underline{1} \\ 1\ 0\ 0\ 0 \end{bmatrix}$$
$$=\theta_1^2+\theta_2-2[2\ 1]=d(\theta_1\theta_2)/dt\ . \tag{25}$$

One obtains θ_4 from the following closed set of rate equations:

$$\frac{d\theta_4}{dt}=\begin{bmatrix} \underline{4} \\ 3\ 2\ 1 \end{bmatrix}=[3\ 2\ 1]-\theta_4=[3\ 2]\theta_1-\theta_4\ , \tag{26}$$

and

$$\frac{d[3\ 2]}{dt}=\begin{bmatrix} \underline{3}\ 2 \\ 2\ 1\ 0\ 0 \end{bmatrix}+\begin{bmatrix} 3\ \underline{2} \\ 2\ 1\ 0\ 0 \end{bmatrix}$$
$$=\begin{bmatrix} \underline{2} \\ 2\ 1\ 0\ 0 \end{bmatrix}+\begin{bmatrix} \underline{3} \\ 2\ 1\ 0 \end{bmatrix}-2[3\ 2]$$
$$=\theta_2^2+\theta_3-2[3\ 2]\neq\frac{d(\theta_3\theta_2)}{dt}\ . \tag{27}$$

One can continue to moderate values of k. The number of *new* equations necessary to determine the θ_k increases by 13, 24, 30, 104, . . . , for θ_5, θ_6, , . . . , θ_8, . . . , respectively. Results are shown in Fig. 6. Note how R_A-R_B approaches zero as time increases (see the insets). The asymptotic growth rate for a $\frac{1}{2}$-sloped vicinal was estimated previously using simulations [8] at roughly 0.33, consistent with the extrapolation in the rightmost inset of Fig. 6.

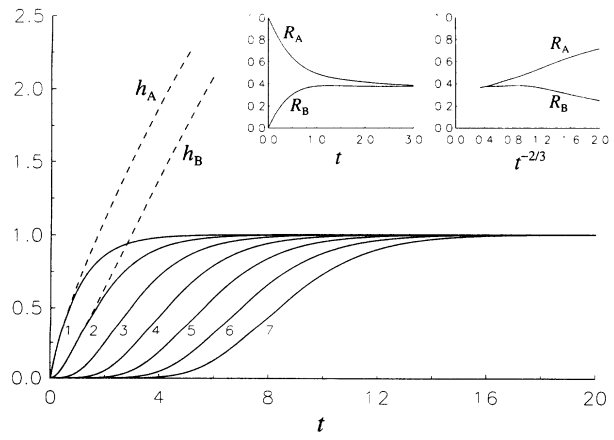

FIG. 6. The coverages of the sites labeled 1–7, and the column heights h_A and h_B, vs time. The insets show the growth rates R_A and R_B vs t (left) and $t^{-2/3}$ (right).

In the case of $d=2+1$, corresponding analysis of the master equations is again possible for various tilt directions (not illustrated here).

B. RSOS growth with larger platforms

One can easily extend our analysis to standard RSOS models with larger platforms. Consider, e.g., the $(d=1+1)$-RSOS model with an n-wide platform (with n odd by symmetry), and the standard single-column height-difference constraint. Here for the layer coverages θ_k with $k\geq 1$, one has the general rate equation

$$\frac{d\theta_k}{dt}=\begin{bmatrix} \underline{k} \\ k-1\ \ k-1\ \ \cdots\ \ k-1\ \ k-1 \end{bmatrix}$$
$$=[k-1\ \ k-1\ \ \cdots\ \ k-1\ \ k-1]-\theta_k\ , \tag{28}$$

where the $(k-1)$-layer platform has always n sites, and $[0]\equiv\theta_0\equiv 1$. Specifically, one calculates

$$\frac{d\theta_1}{dt}=\begin{bmatrix} 1 \\ 0\ \ 0\ \ \cdots\ \ 0\ \ 0 \end{bmatrix}=1-\theta_1\ , \tag{29}$$

$$\frac{d\theta_2}{dt}=\begin{bmatrix} \underline{2} \\ 1\ \ 1\ \ \cdots\ \ 1\ \ 1 \end{bmatrix}$$
$$=[1\ 1\ \cdots\ 1\ 1]-\begin{bmatrix} 2 \\ 1\ \ 1\ \ \cdots\ \ 1\ \ 1 \end{bmatrix}$$
$$=\theta_1^n-\theta_2\ , \tag{30}$$

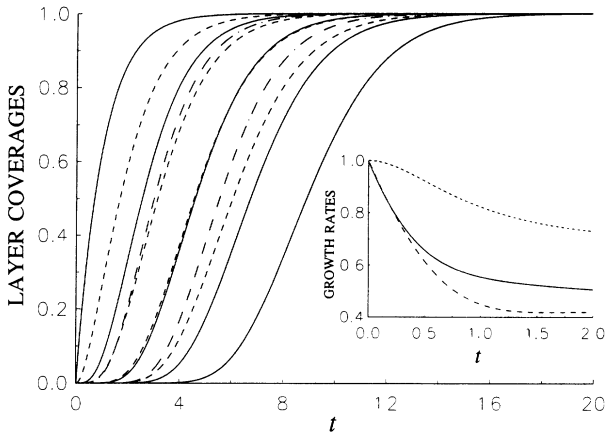

FIG. 7. The first few layer coverages for variations of the standard RSOS model (solid lines) in 1+1 dimensions. Shown are the cases with a double-height constraint and a three-site platform (dashed lines), and the single-height constraint with a five-site platform (dashed-dotted lines). The first layer is the same in all models. The inset shows the corresponding total growth rates. (The dotted line is for the independent-column growth model.)

$$\frac{d\theta_3}{dt}=\begin{bmatrix} & \underline{3} & \\ 2 & 2 \cdots 2 & 2 \end{bmatrix}$$

$$=[2\ 2\ \cdots\ 2\ 2]-\theta_3 \neq \theta_2^n-\theta_3\ ,\ \text{etc}\ . \tag{31}$$

The rate equation for the n-site configuration $[2\ 2\ \cdots\ 2\ 2]$ generates $(n-1)/2$ *new* quantities corresponding to the distinct ways of replacing a 2-site in the sequence by a site of unspecified occupancy. Higher layer coverages are calculated similarly. Brief comparison of the cases $n=5$ and 3 (the later analyzed in Sec. II) is provided in Fig. 7. The $(n=5)$ model is obviously smoother, reflecting the more severe constraint for population of higher layers.

C. RSOS growth with nonunity adjacent column height differences

Less common in studies of nonequilibrium film growth are RSOS models where adjacent columns can differ in height by an integer up to $m>1$. However, as far as writing the hierarchy of master equations, these are simple extensions of the RSOS models with $m=1$. Consider, e.g., the double-height difference model $(m=2)$ in $d=1+1$, with the standard platform constraint $(n=3)$ (see Sec. IV B). The complete set of rate equations for the first four layer coverages is

$$\frac{d\theta_1}{dt}=\begin{bmatrix} & \underline{1} & \\ 0 & 0 & 0 \end{bmatrix}=1-\theta_1\ , \tag{32}$$

$$\frac{d\theta_2}{dt}=\begin{bmatrix} & \underline{2} & \\ & 1 & \\ 0 & 0 & 0 \end{bmatrix}=\begin{bmatrix} & 1 & \\ 0 & 0 & 0 \end{bmatrix}-\begin{bmatrix} & 2 & \\ & 1 & \\ 0 & 0 & 0 \end{bmatrix}$$
$$=\theta_1-\theta_2\ , \tag{33}$$

$$\frac{d\theta_3}{dt}=\begin{bmatrix} & \underline{3} & \\ & 2 & \\ 1 & 1 & 1 \end{bmatrix}=\begin{bmatrix} & 2 & \\ 1 & 1 & 1 \end{bmatrix}-\begin{bmatrix} & 3 & \\ & 2 & \\ 1 & 1 & 1 \end{bmatrix}$$
$$=\begin{bmatrix} & 2 & \\ & 1 & \\ 0 & 0 & 0 \end{bmatrix}\theta_1^2-\theta_3$$
$$=\theta_1^2\theta_2-\theta_3\ , \tag{34}$$

$$\frac{d\theta_4}{dt}=\begin{bmatrix} & \underline{4} & \\ & 3 & \\ 2 & 2 & 2 \end{bmatrix}=\begin{bmatrix} & 3 & \\ 2 & 2 & 2 \end{bmatrix}-\begin{bmatrix} & 4 & \\ & 3 & \\ 2 & 2 & 2 \end{bmatrix}$$
$$=\begin{bmatrix} & 3 & \\ 2 & 2 & 2 \end{bmatrix}-\theta_4\ , \tag{35}$$

where

$$\frac{d\begin{bmatrix} & 3 & \\ 2 & 2 & 2 \end{bmatrix}}{dt}$$
$$=\begin{bmatrix} & \underline{3} & \\ 2 & 2 & 2 \\ 1 & 1 & 1 \end{bmatrix}+2\begin{bmatrix} & 3 & \\ \underline{2} & 2 & 2 \\ 1 & 1 & 1 \end{bmatrix}$$
$$=\begin{bmatrix} 2 & 2 & 2 \\ 1 & 1 & 1 \end{bmatrix}+2\begin{bmatrix} & 3 & \\ & 2 & 2 \\ 1 & 1 & 1 \end{bmatrix}-3\begin{bmatrix} & 3 & \\ 2 & 2 & 2 \end{bmatrix}$$
$$=\theta_2^3+2\begin{bmatrix} & 3 & \\ & 2 & 2 \\ 1 & 1 & 1 \end{bmatrix}-3\begin{bmatrix} & 3 & \\ 2 & 2 & 2 \end{bmatrix}\ , \tag{36}$$

and

$$\frac{d\begin{bmatrix} & 3 & \\ & 2 & 2 \\ 1 & 1 & 1 \end{bmatrix}}{dt}=\begin{bmatrix} & \underline{3} & \\ & 2 & 2 \\ 1 & 1 & 1 \end{bmatrix}+\begin{bmatrix} & 3 & \\ & 2 & \underline{2} \\ 1 & 1 & 1 \end{bmatrix}$$
$$=\begin{bmatrix} & 2 & 2 \\ 1 & 1 & 1 \end{bmatrix}+\begin{bmatrix} & 3 & \\ & 2 & \\ 1 & 1 & 1 \end{bmatrix}-2\begin{bmatrix} & 3 & \\ & 2 & 2 \\ 1 & 1 & 1 \end{bmatrix}$$
$$=\theta_1\theta_2^2+\theta_3-2\begin{bmatrix} & 3 & \\ & 2 & 2 \\ 1 & 1 & 1 \end{bmatrix}\ . \tag{37}$$

Results are shown in Fig. 7, in comparison with the one-dimensional variations discussed above.

A few features are common to the general cases with $n>1$ and $m\geq 1$. One finds, e.g., that all layer coverages $\theta_{1\leq k\leq m}$ satisfy the equation

$$\frac{d\theta_{1\leq k\leq m}}{dt}=\theta_{k-1}-\theta_k\ , \tag{38}$$

where, as before, $\theta_0\equiv 1$, and that

$$\frac{d\theta_{m+1}}{dt}=\theta_1^{n-1}\theta_m-\theta_{m+1}\ . \tag{39}$$

An exact short-time expansion (for finite m and for $n\geq 1$) yields $R(t)=1-t^{m+1}/(m+1)!+\cdots$. The model of independent column growth, for which (38) is satisfied for all k (i.e., the total growth rate equals one at all times), is obtained in the limit when $m\to\infty$ (cf. Fig. 7).

D. Inhomogeneous growth [8,11]

The Wolf-Tang growth technique [11] imposes spatial inhomogeneities in the adsorption rates of certain sites as a way to extract the curvature dependence of the film growth rate (and thus a measure of the kinetic surface tension parameter v). At these sites, growth is either inhibited (and thereby retarded in their vicinity) or enhanced. In spite of the lack of complete translational

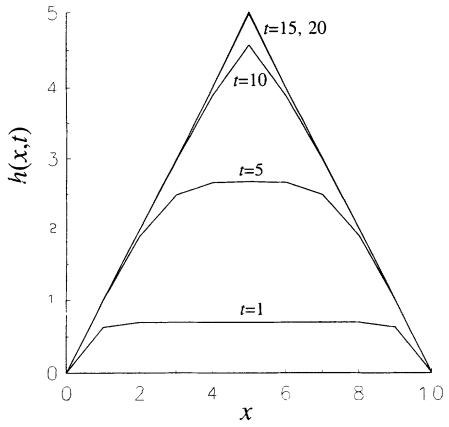

FIG. 8. The average interface profile $h(x,t)$ at successive times for the standard $1+1$-dimensional RSOS model, with deposition forbidden at the sites $x=10k$ with $k=0,\pm1,\pm2,\ldots$

invariance, the early time kinetics can be analyzed via master equations.

Clearly, in the extreme case where deposition is forbidden at defects, the interface becomes pinned. However, for sites which can be filled, the coverages are still determined by the rate equations for a perfect infinite lattice. We exploit this observation to show the profiles for growth until pinning for a model in $d=1+1$ with a periodic array of defects (see Fig. 8).

V. SUMMARY

We have presented an analysis of the early-stage kinetics and some aspects of the structure of a variety of RSOS models of nonequilibrium film growth, with detailed illustrations in $1+1$ and $2+1$ dimensions. This analysis was based on integration of exact finite closed sets of rate equations for the coverages of the first several layers. Although computer simulations remain more efficient to study the asymptotic properties of these models, the exact master equation approach used here is of interest for current experimental situations focusing on the short-time (few-layer) behavior.

ACKNOWLEDGMENTS

This work was supported by National Science Foundation Grant No. CHE-9014214, and was performed at Ames Laboratory. Ames Laboratory is operated for the U.S. Department of Energy by Iowa State University under Contract No. W-7405-Eng-82.

[1] *Dynamics of Fractal Surfaces,* edited by F. Family and T. Vicsek (World Scientific, Singapore, 1991).

[2] *Reflection High-Energy Electron Diffraction and Reflection Imaging of Surfaces,* edited by P. K. Larson and P. J. Dobson (Plenum, New York, 1988).

[3] J. M. Kim and J. M. Kosterlitz, Phys. Rev. Lett. **62**, 2289 (1989); J. M. Kim, J. M. Kosterlitz, and T. Ala-Nissila, J. Phys. A **24**, 5569 (1991); T. Ala-Nissila, T. Hjelt, and J. M. Kosterlitz, Europhys. Lett. **19**, 1 (1992); S. E. Esipov and T. J. Newman, J. Stat. Phys. **70**, 691 (1993).

[4] J. W. Evans, Phys. Rev. B **39**, 5655 (1989).

[5] H. C. Kang and J. W. Evans, Surf. Sci. **271**, 321 (1992).

[6] M. Kardar, G. Parisi, and Y. C. Zhang, Phys. Rev. Lett. **56**, 889 (1986); E. Medina, T. Hwa, M. Kardar, and Y. C. Zhang, Phys. Rev. A **39**, 3053 (1989).

[7] B. M. Forrest and L.-H. Tang, Phys. Rev. Lett. **64**, 1405 (1990); L.-H. Tang, B. M. Forrest, and D. E. Wolf, Phys. Rev. A **45**, 7162 (1992).

[8] H. C. Kang and J. W. Evans, Phys. Rev. A **44**, 2335 (1991).

[9] J. Krug, P. Meakin, and T. Halpin-Healy, Phys. Rev. A **45**, 638 (1992).

[10] J. Krug and P. Meakin, J. Phys. A **23**, L987 (1990).

[11] D. E. Wolf and L.-H. Tang, Phys. Rev. Lett. **65**, 1591 (1990).